Proceedings of the International Conference on Industrial Engineering and Operations Management

Publisher: IEOM Society International, USA DOI: 10.46254/GC03.20260223
Published: February 2, 2026

Quantifying the System-Level Impact of Alkaline Electrolyzer Degradation on Solar-to-Hydrogen Efficiency and Lifetime Performance

Hossam AbdelMeguid
Mechanical Engineering Department, University of Tabuk, Tabuk, Saudi Arabia
Department of Mechanical Power Engineering
Faculty of Engineering, Mansoura University, El-Mansoura, Egypt
habdelmeguid@ut.edu.sa, hssaleh@mans.edu.eg

Abdullah Almubarak, Omar Alotaibi, Abdulrahman Alshaman and Husam Alrehaili
Mechanical Engineering Department
University of Tabuk, Tabuk, Saudi Arabia
431006075@stu.ut.edu.sa, 431002371@stu.ut.edu.sa, 431004604@stu.ut.edu.sa,
hmalrehaili@ut.edu.sa

Abstract

Green hydrogen from solar-powered alkaline water electrolysis (AWE) is pivotal for sustainable energy systems, yet long-term performance predictions often neglect component degradation, leading to overly optimistic feasibility assessments. This paper quantifies the system-level impact of AWE degradation on the lifetime performance of a standalone PV-battery-electrolyzer system. A comprehensive dynamic model was developed, integrating a novel, physics-informed material degradation mechanism based on bubble-induced mechanical stress with coupled sub-models for power generation, storage, and hydrogen production. Comparative "Beginning of Life" (BOL) and 5-year "End of Life" (EOL) simulations were conducted. The results demonstrate that accumulated degradation causes a significant voltage penalty, increasing the AWE cell voltage from 2.0 V to 3.3 V for a 150 W input. In the power-controlled system, this leads to a 41.5% reduction in daily hydrogen throughput. Consequently, the overall solar-to-hydrogen (STH) efficiency collapses from 7.9% at BOL to 4.6% at EOL, an absolute loss of 3.3 percentage points. This study concludes that neglecting AWE degradation leads to a gross overestimation of lifetime productivity, highlighting the necessity of including dynamic aging models in the techno-economic analysis of green hydrogen infrastructure.

Keywords
System-Level Impact, Alkaline Electrolyzer Degradation, Solar-to-Hydrogen Efficiency, Lifetime Performance.

1. Introduction
The global drive toward decarbonization has placed renewable energy and sustainable technologies at the center of energy transition strategies. Among the various clean energy carriers, green hydrogen has emerged as a pivotal solution due to its capacity to decouple energy generation from fossil fuels, thereby reducing greenhouse gas emissions while supporting diverse applications across sectors. Hydrogen produced via renewable-powered electrolysis can serve as a clean fuel for transportation, as a reducing agent in industrial processes such as steel and ammonia production, and as a medium for long-term energy storage that complements the intermittency of solar and wind power. These attributes make hydrogen a cornerstone of emerging low-carbon economies and a critical enabler of sustainable development.

In this context, the Kingdom of Saudi Arabia (KSA) has made substantial commitments to renewable energy deployment, most notably through the NEOM project, which seeks to become a global hub for innovation, sustainability, and green energy (Aljohani et al., 2023). NEOM's unique climatic conditions, characterized by high annual solar radiation (12.54 GJ/m²), moderate wind speeds (15.68 km/h), and favorable temperature ranges (16–38 °C), provide exceptional potential for renewable energy utilization. Studies demonstrate that solar resources in this region can be harnessed not only for electricity production but also for advanced applications including seawater desalination, cooling, and, most importantly, green hydrogen production at rates of 41–47 mol/day/m² (Aljohani et al., 2023). These conditions position NEOM as a leading testbed for large-scale hydrogen initiatives, reflecting broader global efforts to establish sustainable hydrogen economies.

At the technological level, solar-driven electrolysis has been extensively studied as a pathway for cost-effective green hydrogen generation. The integration of photovoltaic (PV) systems with advanced maximum power point tracking (MPPT) controllers and alkaline electrolyzers offers a promising route to maximize energy conversion efficiency and system reliability. Recent modeling studies have highlighted the strong dependence of system performance on solar irradiance variability, underscoring the importance of addressing seasonal fluctuations in hydrogen yield and the need for effective buffering strategies, such as battery storage, to stabilize output (Abdelmeguid et al., 2023; S. AbdelMeguid et al., 2023). These findings emphasize that while the potential of renewable-based hydrogen production is significant, system-level challenges—particularly those related to electrolyzer performance and degradation under variable operating conditions—must be quantitatively assessed to ensure long-term viability and scalability..

1.1 Objectives

The primary goal of this research is to quantify the system-level consequences of material degradation within a standalone, solar-powered alkaline water electrolyzer (AWE) system. To achieve this, the following specific objectives were established:

1. To develop a comprehensive, dynamic system model that integrates a physics-informed material degradation mechanism for the AWE with coupled sub-models for PV power generation, battery storage, and power management.
2. To simulate and compare the system's performance under two distinct scenarios: an ideal 'Beginning of Life' (BOL) state with no degradation, and an aged 'End of Life' (EOL) state after a multi-year operational period with accumulated degradation.
3. To quantify the specific performance losses in the AWE stack attributable to material degradation, including the emergent voltage penalty, the resultant decrease in operating current, and the subsequent reduction in the daily hydrogen production rate.
4. To determine the overall impact on the end-to-end system efficiency by evaluating the absolute reduction in the solar-to-hydrogen (STH) efficiency, thereby demonstrating the necessity of including lifetime performance dynamics in the techno-economic assessment of green hydrogen projects.

2. Literature Review

Alkaline water electrolysis (AWE) remains one of the most mature and commercially relevant technologies for large-scale green hydrogen production due to its robust design, relatively low cost, and independence from scarce noble metals. The process involves the hydrogen evolution reaction (HER) at the cathode and the oxygen evolution reaction (OER) at the anode, with degradation primarily linked to the sluggish kinetics of OER and the long-term stability of electrode materials (Tüysüz, 2023). Structural modifications, phase transformations, and interactions between catalysts and reaction intermediates are known to accelerate degradation, underscoring the importance of durable transition-metal-based electrocatalysts to enhance system longevity and efficiency (Tüysüz, 2023).

Several reviews emphasize that despite its maturity, AWE faces fundamental challenges that hinder its scalability to gigawatt-scale plants. These include electrode degradation, electrolyte and bubble transport inefficiencies, and the need for improved diaphragm or membrane optimization. Addressing these factors is critical for enhancing energy efficiency, reducing capital expenditure, and ensuring dynamic adaptability to intermittent renewable energy sources (Dubouis et al., 2024). Moreover, frequent shutdowns exacerbate degradation by inducing reverse currents and gas crossover, highlighting the importance of improved electrode coatings, thinner diaphragms, and advanced zero-gap designs to operate at higher current densities while maintaining durability (de Groot, 2023).

From a commercialization perspective, achieving stable operation under high current densities while ensuring safety and reliability is essential for market viability. Research identifies stability and safety as critical barriers to large-scale deployment, emphasizing the need for breakthroughs in electrode design and system integration to support future hydrogen economies (Kwon et al., 2023). In parallel, electrode material degradation, particularly at the cathode, has been systematically investigated. Iron-based materials are emerging as cost-effective and stable alternatives, whereas nickel-based electrodes, though widely used, suffer from deterioration under prolonged operation. This highlights the importance of improved material characterization and realistic durability testing beyond conventional thermodynamic predictions such as E–pH diagrams (Esfandiari et al., 2024).

The durability of alkaline water electrolyzers (AWEs) is strongly constrained by electrode degradation under dynamic operating conditions, particularly during frequent start-up and shut-down cycles. Reverse current phenomena have been identified as a critical driver of performance loss, with contrasting effects at the electrodes. At the anode, reverse polarization often enhances oxygen evolution reaction (OER) activity through the formation of $NiOOH/Ni(OH)_2$ species, whereas the cathode suffers severe degradation due to the irreversible oxidation of metallic Ni to $Ni(OH)_2$, leading to reduced hydrogen evolution reaction (HER) activity, conductivity loss, and strain-induced mechanical failure (Wang et al., 2024). Complementary work confirmed that reverse current induces irreversible phase transformations that shorten electrode lifespan, but demonstrated that interrupting ion transfer by lowering electrolyte conductivity during shut-down can effectively mitigate degradation, offering a practical route for enhancing stack durability in renewable-integrated systems (Im et al., 2024).

Start/stop cycling further accelerates degradation in liquid alkaline water electrolyzers (LAWEs), particularly damaging bipolar plates and electrodes under reverse current conditions. Laboratory-scale investigations have shown that while start/stop strategies can partially replicate these effects, the extrapolation to industrial stacks remains uncertain, underscoring the need for improved understanding of scale-dependent degradation processes (Maurya et al., 2024). Catalyst layer degradation during shut-down is another major limitation, with conventional uncatalyzed Ni anodes exhibiting poor reverse-current tolerance and mechanical instability. This highlights the necessity of developing reverse-current-tolerant catalyst layers tailored for fluctuating renewable energy inputs to maintain high efficiency and extend electrolyzer lifetime (Lindquist, 2024).

In industrial-scale AWEs, iron electrodeposition has been identified as a dominant degradation pathway, reducing HER activity and increasing ohmic overpotential by altering membrane porosity and electrode surfaces. A validated multiphysics model confirmed the significance of this mechanism, showing strong agreement with experimental data (±3%) and enabling the coupling of degradation effects with economic analysis. The findings emphasize that operational strategies minimizing iron contamination and deposition are essential for sustaining long-term efficiency and cost-effectiveness in large-scale hydrogen production (Huang et al., 2024).

Beyond these electrochemical pathways, material design significantly influences degradation resistance. Recent studies on electrodeposited nickel electrodes have highlighted the role of morphology in mitigating corrosion. Bulk and mesoporous (MP) nickel electrodes exposed to alkaline electrolysis showed improved stability under magnetic fields, attributed to reduced gas bubble adhesion and stabilization of the hydroxide layer. Notably, mesoporous Ni electrodes exhibited markedly less structural damage, owing to their high density of active sites and inherent porosity, which minimized bubble-induced stress and surface deterioration. While large-scale application of magnetic field-assisted electrolysis poses economic and technical challenges, the use of mesoporous nickel electrodes offers a promising pathway to enhance durability and efficiency in AWEs (Farmani et al., 2025).

The integration of alkaline water electrolyzers (AWEs) with renewable energy systems necessitates robust dynamic performance to accommodate fluctuating inputs. At the pilot scale, a 25 kW AWE demonstrated rapid ramp-up times, achieving optimal system efficiency of 64% at 52 A stack current, with hydrogen flow rate exhibiting exponential dependence on current. These results underscore the potential of AWEs for renewable-powered applications, though techno-economic analysis revealed relatively high levelized cost of hydrogen (LCOH), highlighting the need for further cost optimization (Bora, 2025). At the industrial scale, experimental studies on a 250 kW system revealed complex response characteristics during start-stop and variable load operations across seconds to hours, with performance strongly influenced by transient current, voltage, temperature, and gas crossover dynamics. The findings provide essential guidelines for designing control strategies that enhance operational stability under intermittent renewable supply (Gu et al., 2023).

Complementary modeling studies have advanced the predictive understanding of dynamic AWE operation. A detailed model incorporating cell voltage, electrolyte concentration, temperature, and gas purity achieved high accuracy for laboratory systems, but its predictive capacity diminished for industrial stacks exceeding 1 m² active area due to limitations in the assumption of perfectly mixed half-cells. Improved models incorporating height-dependent gas fraction distributions are therefore critical for capturing large-scale performance under dynamic renewable coupling (Turek et al., 2024). Parallel analyses of safety and efficiency challenges emphasize that renewable-driven wide-range operation can compromise gas purity, power regulation flexibility, and long-term efficiency. Addressing these issues requires mechanism-based approaches to identify degradation pathways and operational limits, as well as improved design strategies for enhanced system reliability (Haoran et al., 2024).

In summary, the durability of alkaline water electrolyzers is constrained by electrochemical degradation mechanisms such as reverse current-induced Ni oxidation, contamination-driven electrodeposition, and mechanical stress from bubble formation, which collectively impair efficiency and reliability. Recent advances—including reverse-current mitigation strategies, improved dynamic operation models, and the development of mesoporous Ni electrodes—demonstrate promising pathways to enhance stability and efficiency. However, scaling these solutions to industrial systems remains a key challenge, requiring integrated approaches that couple material innovation with optimized operational control for reliable renewable-powered hydrogen production.

2.1 Research Question

This study seeks to investigate the extent to which progressive material degradation in alkaline water electrolyzers influences the long-term operational performance of standalone, PV driven green hydrogen systems. Specifically, the analysis focuses on quantifying how electrode and component degradation mechanisms affect two critical performance indicators: the daily hydrogen production rate and the overall solar-to-hydrogen (STH) efficiency.

2.2 Research Gap

Despite extensive advancements in AWE, several gaps remain in understanding and addressing degradation mechanisms, dynamic operation under renewable intermittency, and long-term integration with PV-driven systems. Table 1 summarizes the critical research gaps identified.

Table 1. Summary of Research Gaps in Alkaline Water Electrolyzer Durability, Dynamic Operation, and PV-Integrated Green Hydrogen Systems.

Area	Current Understanding	Identified Gap	Implication
Degradation & Durability	Reverse current during start/stop cycles causes severe cathode oxidation and electrode failure; mesoporous Ni electrodes improve resilience (Huang et al., 2024; Im et al., 2024; Lindquist, 2024; Maurya et al., 2024; Wang et al., 2024)	Lack of quantitative link between progressive material degradation and hydrogen output/efficiency over long-term operation.	Limits predictive durability models and techno-economic optimization.
Dynamic Operation	Pilot-scale studies (25 kW and 250 kW) demonstrate rapid ramp-up and variable load response (Bora, 2025; Gu et al., 2023).	Insufficient models for scaling dynamic behavior to industrial stacks, especially under fluctuating renewable input.	Uncertainty in system design and control strategies for grid-independent operation.
System Integration with Renewables	Models highlight efficiency and gas purity challenges during part-load operation and safety risks from impurity accumulation ([22], [26]).	Limited experimental validation of AWE behavior in real standalone PV-powered systems with daily/seasonal solar variability.	Knowledge gap hampers reliable PV–AWE coupling for decentralized hydrogen production.
Materials & Catalysts	Research suggests reverse-current tolerant catalysts and mesoporous structures improve durability	Lack of scalable, cost-effective electrode materials validated under	Constrains commercialization and large-scale deployment.

	(Farmani et al., 2025; Lindquist, 2024)	industrial cycling and harsh environments.	
Techno-Economic Analysis	LCOH for pilot plants remains high; economic models consider efficiency but rarely incorporate degradation effects (Bora, 2025; Huang et al., 2024)	Absence of integrated degradation–performance–cost models linking material aging with hydrogen cost projections.	Prevents accurate assessment of system viability over 10–20 year lifetimes.

3. System Modeling and Methodology

To quantify the long-term performance of a standalone green hydrogen system, a comprehensive dynamic simulation model was developed in MATLAB. This model integrates the interdependent behaviors of each key subsystem: solar energy conversion, power management and storage, and hydrogen generation via alkaline water electrolysis. This section details the architecture of the simulated system and the mathematical models governing each component..

3.1 System Architecture

The simulated system, depicted in Figure 1, represents a typical off-grid green hydrogen production facility. It comprises four primary subsystems:

- **A Photovoltaic Panel:** Captures solar irradiance and converts it into DC electrical power.
- **A Maximum Power Point Tracking (MPPT) Controller:** Manages the flow of energy, optimizing power extraction from the PV panel and directing it to the load or battery.
- **A Battery Storage System:** Acts as an energy buffer, storing surplus solar energy for later use and supplying power during periods of low irradiance to maintain stable operation of the electrolyzer.
- **An Alkaline Water Electrolyzer Stack:** The primary load, which consumes DC power to produce hydrogen gas through the electrolysis of an aqueous alkaline solution.

The model simulates the dynamic response of this integrated system to a time-varying environmental profile of solar irradiance and ambient temperature, with a temporal resolution of 60 seconds.

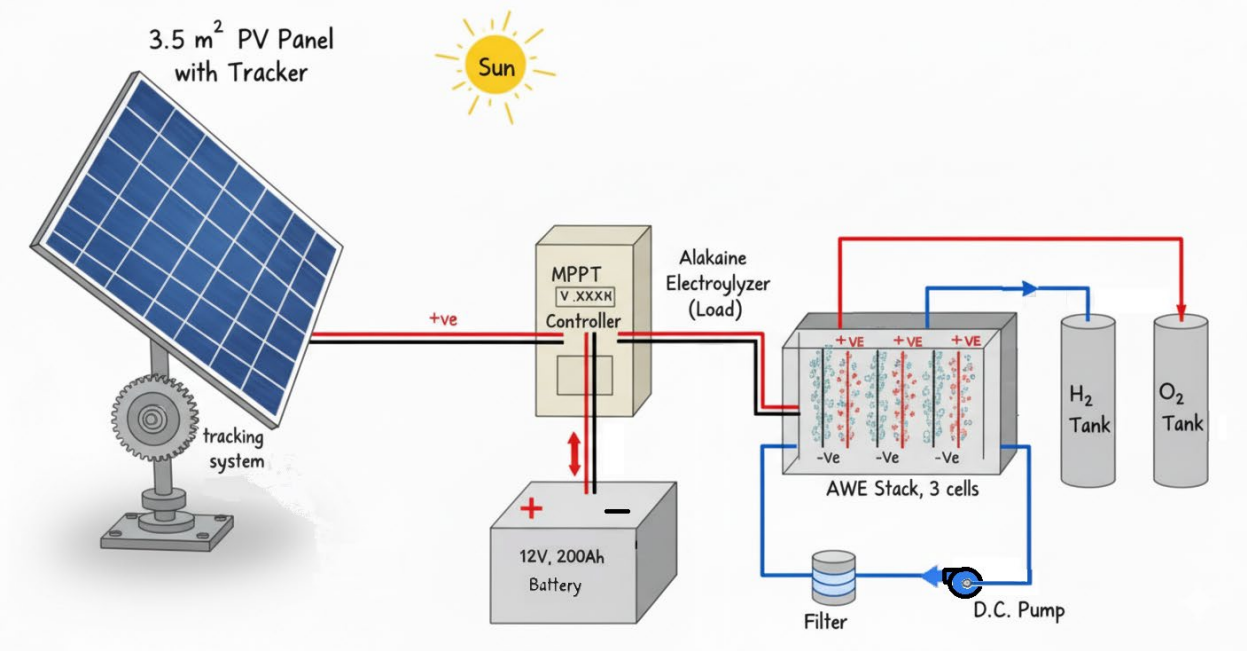

Figure 1. The system diagram of a standalone, off-grid solar-to-hydrogen production unit

3.2. Integrated Mathematical Models

The system is described by a set of coupled differential and algebraic equations.

PV Panel Electrical Model

The power output of the PV panel (P_pv) is modeled using the single-diode equivalent circuit approach. The current-voltage (I-V) characteristic is given by:

$$I_{pv} = I_{ph} - I_0\left[\exp\left(\frac{V_{pv} + I_{pv}R_s}{nV_t}\right) - 1\right] - \frac{V_{pv} + I_{pv}R_s}{R_{sh}} \quad (1)$$

where:

I_{pv}, V_{pv}: Output current and voltage of the panel.

I_{ph}: Photocurrent, proportional to solar irradiance G.

$$I_{ph} = \left[I_{sc,ref} + K_i(T_{cell} - T_{ref})\right]\frac{G}{G_{ref}}$$

I_0: Diode reverse saturation current, strongly dependent on cell temperature.

R_s, R_{sh}: Series and shunt resistances.

n: Diode ideality factor.

$V_t = kT_{cell}/q$: Thermal voltage.

The MPPT controller continuously adjusts I_{pv} and V_{pv} to maximize the output power. $P_{pv} = V_{pv} \times I_{pv}$

PV Panel Thermal Model

The cell temperature T_{cell} is crucial for accuracy and is determined by a thermal energy balance:

$$mc_p \frac{dT_{cell}}{dt} = A_{pv} I(\tau\alpha) - P_{pv} - U_L A_{pv}(T_{cell} - T_{amb}) \quad (2)$$

where:

mc_p: Thermal mass of the panel.

A_{pv}: Panel area.

$\tau\alpha$: Effective transmittance-absorptance product.

U_L: Overall heat loss coefficient, often modeled as a function of wind speed V_{wind}.

Battery Model

The State of Charge (SOC) is modeled using coulomb counting, which integrates the battery current (I_{bat}):

$$\mathrm{SOC}(t) = \mathrm{SOC}(t_0) - \int_{t_0}^{t} \frac{\eta_{bat} I_{bat}(\tau)}{C_{bat}} d\tau \quad (3)$$

where:

C_{bat}: Nominal battery capacity.

I_{bat}: Battery current (positive for discharging, negative for charging).

η_{bat}: Coulombic efficiency (different for charging and discharging).

Power Management Logic (MPPT Controller)

The controller dictates the power flow. The electrolyzer power demand is $P_{elec} = V_{cell} \times I_{elec}$.

$$\begin{aligned}
&If\ P_{pv} > P_{elec} \text{ and } \mathrm{SOC} < 100\% \quad : I_{bat} = I_{elec} - I_{pv} \quad \text{(Battery charges).} \\
&If\ P_{pv} > P_{elec} \text{ and } \mathrm{SOC} = 100\% \quad : P_{pv} \text{ is curtailed to match } P_{elec} \text{ (or } P_{elec} \text{ is increased if possible).} \\
&If\ P_{pv} < P_{elec} \text{ and } \mathrm{SOC} > \mathrm{SOC}_{min} : I_{bat} = I_{elec} - I_{pv} \quad \text{(Battery discharges).} \\
&If\ P_{pv} < P_{elec} \text{ and } \mathrm{SOC} \le \mathrm{SOC}_{min} : P_{elec} \text{ is reduced or the system shuts down, } I_{elec} = 0.
\end{aligned} \quad (4)$$

Alkaline Electrolyzer (AWE) Stack Model

This is a multi-physics model based on the work of (Farmani et al., 2025; Hu et al., 2022). The total voltage across a single cell V_{cell} is the sum of the reversible potential and various overpotentials:

$$V_{cell}(J,T_{stack}) = V_{rev}(T_{stack},P) + V_{act,a}(J,T_{stack}) + V_{act,c}(J,T_{stack}) + V_{ohm}(J,T_{stack},\alpha_g) \quad (5)$$

Reversible Voltage (V_{rev}): The minimum thermodynamic voltage required.

$$V_{rev} = V_{rev}^{0} + \frac{RT_{stack}}{2F}\ln\left(\frac{a_{H_2}a_{O_2}^{0.5}}{a_{H_2O}}\right) \quad (6)$$

Activation Overpotential (V_{act}): Energy barrier for the electrochemical reactions, modeled using the Butler-Volmer equation, often simplified to the Tafel equation at higher current densities ($J = I_{elec} / A_{elec}$).

$$V_{act,k} = \frac{RT_{stack}}{\alpha_k nF}\sinh^{-1}\left(\frac{J}{2j_{0,k}(1-\alpha_g)}\right) \approx a_k + b_k \log\left(\frac{J}{1-\alpha_g}\right) \quad (7)$$

where k denotes anode (a) or cathode (c), j_0 is the exchange current density, and the term (1-α_g) accounts for the reduction in effective electrode area due to gas bubbles (void fraction).

Ohmic Overpotential (V_{ohm}): Voltage drop due to resistance in the electrodes, electrolyte, and diaphragm. This is where degradation has a major impact.

$$V_{ohm} = J \cdot (R_{elec} + R_{ion} + R_{mem} + R_{bubble}(\alpha_g) + R_{deg}(t)) \quad (8)$$

The void fraction α_g represents the volume fraction of gas bubbles in the electrolyte channels. It directly impacts both activation and ohmic overpotentials. We adapt the bubble coverage rate model from (Hu et al., 2022). as a proxy for α_g:

$$\alpha_g = 0.023 \cdot J^{0.3}\left(\frac{T_{ref}}{T_{stack}}\right)\left(\frac{P_{ref}}{P}\right) \quad (9)$$

This semi-empirical model captures the key dependencies: α_g increases with current density J but decreases with higher stack temperature T_{stack} and operating pressure P.

The dynamic stack temperature is governed by a lumped-parameter energy balance:

$$C_{th,stack}\frac{dT_{stack}}{dt} = \dot{Q}_{gen} - \dot{Q}_{loss} - \dot{Q}_{react} \quad (10)$$

Heat Generation ($\dot{Q}_{gen}$): Primarily from overpotentials.

$$\dot{Q}_{gen} = N_{cells} \cdot I_{elec} \cdot (V_{cell} - V_{tn}) \quad (11)$$

where V_{tn} is the thermoneutral voltage.

Heat Loss ($\dot{Q}_{loss}$): Convective and radiative losses to the environment.

$$\dot{Q}_{loss} = hA_{stack}(T_{stack} - T_{amb}) \quad (12)$$

Heat Removed by Reactants/Products ($\dot{Q}_{react}$): Enthalpy change of the flowing water, H_2, and O_2 streams.

Material Degradation Model

The novel contribution of this work lies in the integration of a dynamic material degradation model. Based on the findings of (Farmani et al., 2025)., which identify bubble-induced mechanical stress as a primary driver of degradation in Ni-based alkaline electrodes, we model degradation as a progressive increase in the cell's ohmic resistance (R_{deg}). The rate of this increase is a function of the primary operational stressors: current density (J), bubble void fraction (α_g:), and stack temperature (T_{stack}). The degradation rate is expressed as:

$$\frac{dR_{deg}}{dt} = k_{deg} \cdot J^{n} \cdot (\alpha_g)^{m} \cdot \exp\left(-\frac{E_{a,deg}}{RT_{stack}}\right) \quad (13)$$

where k_{deg} is the intrinsic degradation rate constant, n and m are exponents defining the sensitivity to current density and void fraction respectively, and $E_{a,deg}$ is the activation energy for the degradation processes. This rate is integrated over the simulation time to yield the total accumulated degradation resistance, $R_{deg}(t)$, which directly impacts the ohmic overpotential as shown in Eq (8).

3.3 Simulation and Analysis Framework

To quantify the impact of degradation, a comparative study was performed. First, a "Beginning of Life" (BOL) simulation was conducted over a 48-hour period with the degradation model disabled (k_{deg} = 0). Second, an "End of Life" (EOL) simulation was run for a 5-year period with the full degradation model enabled. The performance on the

final day of the EOL simulation was then directly compared against the BOL results to isolate and quantify the long-term performance losses. Key system parameters for the simulation are listed in Table 2

Table 2. Key Parameters for the Integrated Green Hydrogen System Simulation.

Category	Parameter	Symbol	Value	Units
PV Panel	Panel Area	A_{pv}	3.5	m²
	Reference Short-Circuit Current	$I_{sc,ref}$	6.1	A
	Reference Open-Circuit Voltage	$V_{oc,ref}$	22.5	V
	Temperature Coeff. of I sc	K_i	0.0032	A/K
	Diode Ideality Factor	n	1.3	-
	Series Resistance	R_s	0.221	Ω
	Shunt Resistance	R_{sh}	415	Ω
	Heat Loss Coefficient	U_L	20	W/(m²·K)
Battery	Nominal Capacity	C_{nom}	200	Ah
	Nominal Voltage	V_{nom}	12	V
	Charging Efficiency	η_{ch}	95%	-
	Discharging Efficiency	η_{dch}	90%	-
	Minimum State of Charge	SoC_{min}	20%	-
	Maximum State of Charge	SoC_{max}	90%	-
AWE Stack	Number of Cells	N_{cells}	3	-
	Nominal Operating Power	$P_{nominal}$	150	W
	Electrode Area per Cell	A_{elec}	0.04	m²
	Initial Ohmic Resistance	$R_{ohm,initial}$	0.003	Ω·m²
	Thermal Mass	C_{th}	5000	J/K
	Heat Loss Coefficient	h_{loss}	4	W/(m²·K)
Degradation Model	Rate Constant	k_{deg}	1.0 x 10^{-12}	(units vary)[1]
	Current Density Exponent	n	1.5	-
	Void Fraction Exponent	m	1.0	-
	Activation Energy	$E_{a,deg}$	20,000	J/mol

[1] *Units for k_deg are complex, e.g., $(\Omega \cdot m^2)/s \cdot (A/m^2)^{-n}$.*

3.4 Performance Evaluation Metrics

To provide a comprehensive and quantitative assessment of the system's performance and the impact of degradation, several Key Performance Indicators (KPIs) were defined and calculated throughout the simulation. These metrics evaluate the performance at the component, subsystem, and overall system levels.

Daily Hydrogen Production

The primary measure of the system's output is the total mass of hydrogen produced over a 24-hour operational cycle. It is calculated by integrating the instantaneous hydrogen production rate ($\dot{m}_{H2}$) over the duration of one day:

$$m_{H2,daily} = \int_{day\_start}^{day\_end} \dot{m}_{H2}(t)dt \tag{14}$$

Where $\dot{m}_{H2}$ is derived from the electrolyzer current via Faraday's Law. This metric directly reflects the system's throughput and is a key indicator of performance loss due to degradation.

Electrolyzer Electrical Efficiency

The electrical efficiency, or Voltaic efficiency (η_{elec}), of the AWE stack quantifies how effectively the consumed electrical energy is used for the water-splitting reaction, compared to the minimum theoretical energy required. It is defined as:

$$\eta_{elec}(t) = \frac{V_{tn}}{V_{cell}(t)} \tag{15}$$

Solar-to-Hydrogen (STH) Efficiency

The Solar-to-Hydrogen (STH) efficiency is the ultimate "sunlight-to-fuel" metric for the entire system. It represents the ratio of the chemical energy stored in all the hydrogen produced up to a given time (t) to the total solar energy that

has impinged on the PV panel area over the same period. It is calculated using the Lower Heating Value of hydrogen (LHV_{H2}):

$$\eta_{STH}(t) = \frac{m_{H2,accum}(t) \times LHV_{H2}}{\int_0^t G(t) \cdot A_{pv} \cdot d\tau} \tag{16}$$

where $m_{H2,\,accum}(t)$ is the cumulative mass of hydrogen produced, G(t) is the instantaneous solar irradiance,. This KPI holistically accounts for all losses in the system, from PV conversion and power electronics to battery round-trip losses and electrolyzer inefficiencies. The average operational STH efficiency over a single day is used for comparing BOL and EOL performance.

Voltage Penalty and Current Drop

To specifically isolate the electrical impact of degradation, two differential metrics are defined by comparing the performance on the final day of the End of Life (EOL) simulation to the Beginning of Life (BOL) baseline:

Voltage Penalty (ΔV): The increase in the peak operating cell voltage at EOL compared to BOL. This directly quantifies the impact of the accumulated degradation resistance (R_{deg}).

$$\Delta V = V_{cell,peak,EOL} - V_{cell,peak,BOL} \tag{17}$$

Current Drop ($\Delta I_{\%}$): The percentage reduction in the peak operating current at EOL compared to BOL, which occurs as a consequence of the voltage penalty in the power-controlled system.

$$\Delta I_{\%} = \left(1 - \frac{I_{awe,peak,EOL}}{I_{awe,peak,BOL}}\right) \times 100\% \tag{18}$$

Together, these metrics provide a clear picture of the electrochemical performance decay of the AWE stack.

5. Results and Discussion

The dynamic simulation model was executed for both the Beginning of Life (BOL) and the 5-year End of Life (EOL) scenarios to quantify the performance impacts of AWE degradation. This section presents and discusses the key findings, beginning with the environmental inputs that drive the system's operation.

5.1 Environmental Operating Conditions

The performance of the solar-powered system is fundamentally dictated by the diurnal patterns of solar irradiance and ambient temperature. Figure 2 illustrates the standardized 24-hour environmental profile used for each day of the simulation to ensure a consistent basis for comparison between the BOL and EOL states.

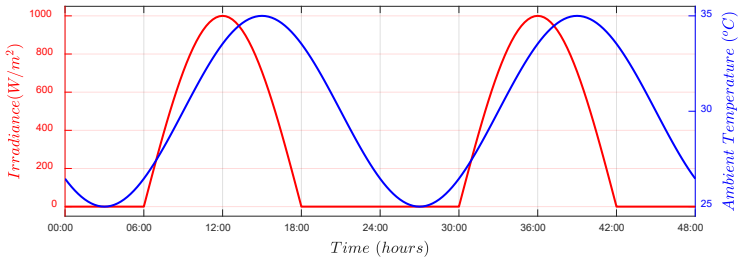

Figure 2. Diurnal Profile of Solar Irradiance and Ambient Temperature.

The solar irradiance profile begins at 06:30, peaks at 1000 W/m² at noon, and declines to zero by 18:00, yielding a total daily insolation of 7.8 kWh/m² under clear sky conditions. The ambient temperature follows a sinusoidal pattern, ranging from a nocturnal minimum of 25.0 °C to a diurnal maximum of 35.0 °C in the late afternoon. These controlled daily inputs—irradiance and temperature—ensure that performance variations between the BOL and EOL electrolyzer scenarios arise exclusively from material degradation effects.

5.2 System Power Management and Energy Flow

The MPPT controller and battery storage system are responsible for mediating the variable solar power generation to provide a stable input to the electrolyzer. Figure 3 details the dynamic power flows between the PV panel, battery, and AWE load over a 48-hour period, demonstrating the controller's energy management strategy.

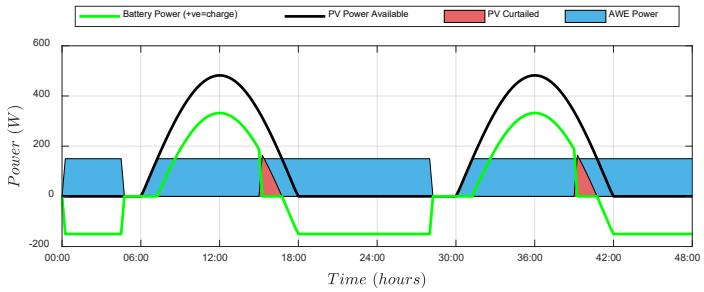

Figure 3. System Power Flow Dynamics

The simulation results demonstrate the effectiveness of the hybrid PV–battery power management strategy in ensuring continuous operation of the alkaline water electrolyzer (AWE) at its nominal demand of 150 W. During the night period (00:00–06:00), when no solar energy is available, the battery exclusively supplies the electrolyzer, discharging at a nearly constant rate of 150 W. As sunrise begins (06:30–07:30), PV generation gradually increases but remains insufficient to meet the electrolyzer demand; thus, the battery compensates for the shortfall, with the maximum deficit recorded at –30.6 W at 17:00.

Once solar irradiance reaches higher levels (07:30–15:30), PV output exceeds the electrolyzer demand, and the excess power is directed to battery charging. The charging rate peaks at 332.2 W at noon, ensuring rapid recovery of the battery's state of charge. By 15:30–16:30, the battery becomes fully charged, and any additional PV generation that cannot be utilized is curtailed, as illustrated by the case where PV output of 289.5 W led to –139.5 W being curtailed. This curtailment highlights the limitation of the system in handling surplus energy once storage reaches capacity.

5.3 Impact of Degradation on AWE Performance and Throughput

The core of this investigation is to quantify the performance decay of the AWE stack resulting from long-term material degradation. By directly comparing the operational data from the Beginning of Life (BOL) and End of Life (EOL) scenarios under identical power inputs, the specific impacts on voltage, current, internal dynamics, and hydrogen production are isolated. Figure 4 presents this comparative analysis.

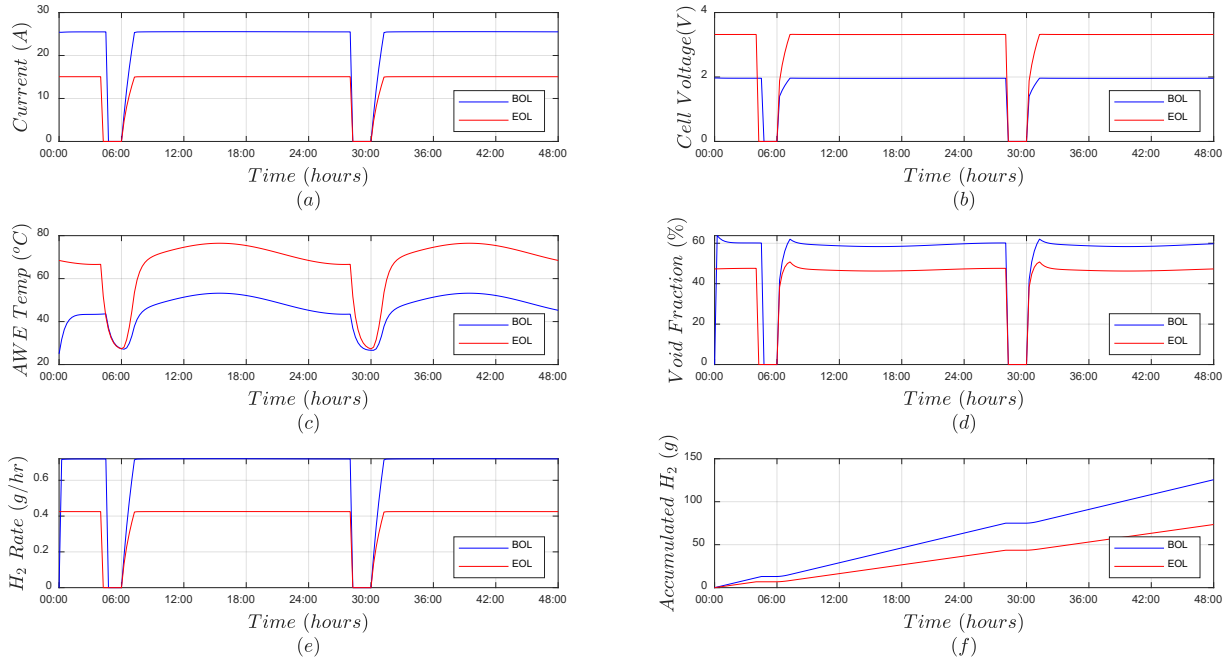

Figure 4. Comparative AWE Performance at BOL vs. EOL. (a) Operating current, (b) Cell voltage, (c) Stack temperature, (d) Bubble void fraction, (e) Instantaneous H_2 production rate, and (f) Cumulative H_2 production.

The simulation results reveal a significant cascade of performance degradation. As shown in Figure 4(b), the aged electrolyzer (EOL) exhibits a substantial voltage penalty, consistently operating at a cell voltage of approximately 3.3 V, compared to the 2.0 V of the new electrolyzer (BOL) for the same 150 W power input. This increased internal resistance is the primary manifestation of the accumulated material degradation.

This voltage penalty directly impacts the operational current, as the system is power-controlled. Figure 4(a) demonstrates that the EOL stack draws a significantly lower current (peak 15.1 A) compared to the BOL stack (peak 25.5 A), representing a current drop of approximately 41%. This reduction in current has a direct and detrimental effect on the electrolyzer's primary function. According to Faraday's Law, the hydrogen production rate is proportional to current, and this is clearly observed in Figure 4(e). The EOL system's H_2 production rate is reduced to approximately 0.4 g/hr, a stark decrease from the 0.7 g/hr achieved by the BOL system.

The degradation also has thermal consequences. The higher voltage at EOL leads to greater resistive heating, causing the stack to operate at a significantly higher temperature (peak ~76 °C) compared to the BOL stack (peak ~53 °C), as seen in Figure 4(c). This higher temperature, in turn, affects the two-phase flow dynamics, resulting in a lower bubble void fraction at EOL (~47%) versus BOL (~60%), as shown in Figure 4(d).

Ultimately, the most critical impact is on the total system output. Figure 4(f) illustrates the cumulative hydrogen production over the 48-hour period. The BOL system produced approximately 125.6 g of hydrogen, whereas the degraded EOL system produced only 73.5 g under identical solar and power input conditions. This represents a total production loss of 41.5%, starkly quantifying the profound system-level impact of long-term material degradation.

5.4 Thermal Implications of Long-Term Degradation

The increase in internal ohmic resistance due to material degradation directly impacts the thermal behavior of the AWE stack. As electrical efficiency decreases, a larger fraction of the input energy is converted into waste heat. Figure 5 illustrates the comparative heat generation and heat loss rates for the BOL and EOL scenarios, highlighting the significant thermal stress placed on the aged system.

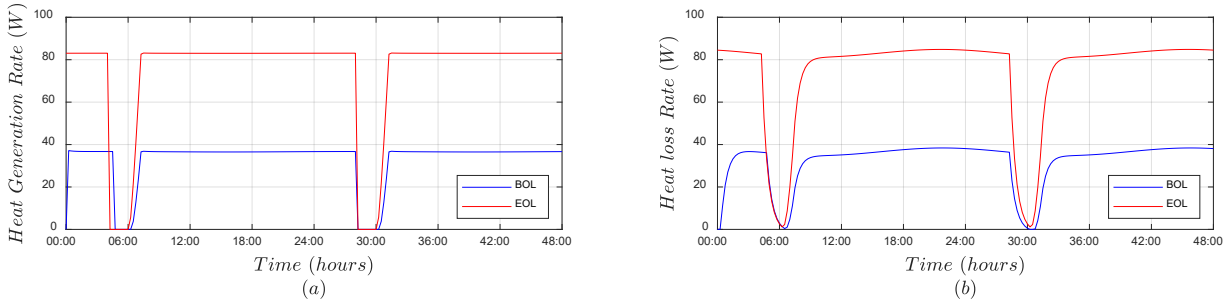

Figure 5. Comparative Thermal Dynamics at Beginning of Life (BOL) vs. End of Life (EOL). (a) Instantaneous heat generation rate within the AWE stack, and (b) Heat loss rate from the stack to the ambient environment.

The results reveal that the degraded EOL electrolyzer operates under a significantly higher thermal load compared to the BOL stack. At the same 150 W input, the EOL stack produces 83.1 W of waste heat, more than double the 36.7 W generated by the BOL stack, reflecting reduced electrical efficiency due to higher overpotentials. Consequently, the EOL stack equilibrates at a higher operating temperature, with heat losses (~84 W) closely matching its increased heat generation, compared to ~37 W in the BOL case. This establishes a feedback mechanism where degradation amplifies heat generation, elevates temperature, and further accelerates material deterioration, highlighting the critical role of thermal management in prolonging electrolyzer durability.

5.5 Long-Term Impact on System and Component Efficiency

The cumulative effect of material degradation is most critically observed in the long-term decay of the system's overall efficiency. By tracking both the AWE electrical efficiency and the end-to-end solar-to-hydrogen (STH) efficiency over the simulated 5-year operational period, the full scope of the performance decline can be quantified. Figure 6 presents the evolution of these two key efficiency metrics.

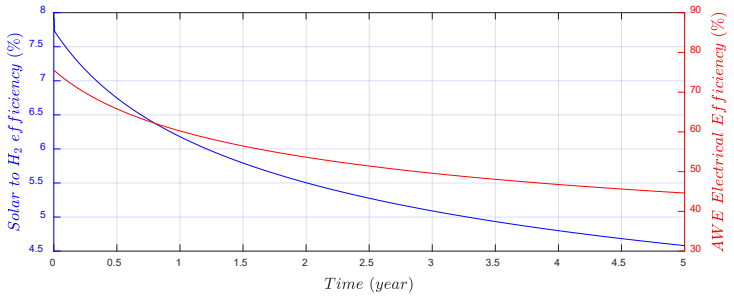

Figure 6. Long-Term Efficiency Degradation over a 5-Year Period.

The simulation results indicate a pronounced and continuous degradation in system performance over a five-year period. At the component level, the AWE stack's electrical efficiency declines from an initial 75.5% at BOL to only 44.6% after five years, corresponding to an absolute loss of about 31 percentage points. This reflects the increasing internal resistance, where a progressively larger fraction of the input power is dissipated as waste heat rather than being converted to hydrogen. At the system scale, the solar-to-hydrogen (STH) efficiency mirrors this decay, decreasing from 7.9% at BOL to 4.6% at EOL, an absolute drop of 3.3 percentage points. This means the system retains only 58% of its original effectiveness in converting solar energy to hydrogen after five years. These findings highlight the critical influence of material degradation on long-term performance and emphasize that failing to account for degradation leads to significant overestimation of hydrogen yield and overall viability of PV-powered electrolysis systems.

5.6 Discussion

The simulation results provide a clear, quantitative narrative of how component-level material degradation cascades into significant system-level performance losses over a 5-year operational period. The initial manifestation of aging is an increase in the AWE's internal ohmic resistance, which forces a substantial voltage penalty to maintain the

nominal 150 W power input. As demonstrated, this higher operating voltage (3.3 V at EOL vs. 2.0 V at BOL) directly reduces the electrolyzer's current draw by approximately 41% in the power-controlled system.

This current reduction has immediate and critical consequences, as predicted by Faraday's Law. The daily hydrogen throughput of the aged system was found to be 41.5% lower than that of the new system under identical environmental and power input conditions. This loss of production is the most direct measure of the degradation's impact on the system's primary function.

Furthermore, the increased voltage penalty directly translates to lower electrical efficiency and greater thermal stress. The AWE's electrical efficiency plummeted from 75.5% to 44.6%, with the excess energy manifesting as a more than twofold increase in waste heat generation. This elevated thermal load not only represents a loss of useful energy but also creates a potential feedback loop, as higher operating temperatures can accelerate the very degradation mechanisms causing the inefficiency.

Ultimately, these compounding losses culminate in a severe decline in the overall system's effectiveness. The end-to-end solar-to-hydrogen efficiency—the definitive metric for a green hydrogen system—was reduced from 7.9% to 4.6%. This finding underscores the central conclusion of this study: neglecting the progressive and cumulative effects of material degradation can lead to a significant overestimation of the long-term viability and hydrogen output of such systems. The results strongly advocate for the inclusion of dynamic degradation models in the techno-economic assessment and design optimization of future green hydrogen infrastructure.

6. Conclusion

This study successfully quantified the system-level impact of progressive material degradation on the long-term performance of a standalone, solar-powered green hydrogen system. By integrating a novel, physics-informed degradation model into a comprehensive dynamic simulation, a comparative analysis between BO) and 5-year EOL performance was conducted. The results unequivocally demonstrate that component aging is a critical factor that significantly curtails the lifetime productivity and efficiency of such systems.
The key findings of this research are summarized as follows:

- Significant Voltage Penalty: Material degradation, modeled as an increase in ohmic resistance, resulted in a substantial voltage penalty, with the AWE cell voltage increasing from 2.0 V to 3.3 V under a nominal 150 W power input over a 5-year period.
- Reduced Hydrogen Throughput: In the power-controlled system, the higher voltage directly led to a 41% reduction in operating current, which consequently caused the daily hydrogen production to decrease by 41.5% from BOL to EOL.
- Increased Thermal Load: The loss in electrical efficiency manifested as a significant increase in thermal stress, with the degraded AWE generating more than twice the amount of waste heat (83.1 W at EOL vs. 36.7 W at BOL) for the same electrical input.
- System-Level Efficiency Collapse: The compounding component-level losses culminated in a severe decline in the overall system's end-to-end effectiveness. The solar-to-hydrogen (STH) efficiency fell from 7.9% at BOL to 4.6% at EOL, representing an absolute loss of 3.3 percentage points and a relative performance drop of over 40%.

This work highlights the critical necessity of incorporating dynamic degradation effects into the predictive models used for designing and evaluating green hydrogen projects. Neglecting the realities of component aging leads to a significant overestimation of lifetime hydrogen output and economic viability. The modeling framework presented herein provides a robust tool for more realistic techno-economic analysis, for the development of degradation-aware control strategies, and for the optimization of system designs that balance initial performance with long-term operational longevity.

References

Abdelmeguid, H., Al-Johani, H., Saleh, Z., Almalki, A., and Almalki, A., “Advancements in Green Hydrogen Production using Seawater Electrolysis in Tabuk, Saudi Arabia,” International Journal of Engineering (IJE), vol. 15, no. 3, pp. 42–55, 2023.

Aljohani, Z., Asiri, A., Al-awlaqi, S., Aljohani, T., and Abdelmeguid, H., “Assessment of Solar Energy Availability and Its Potential Applications in NEOM Region,” Renewable Energy Research and Applications (RERA), vol.

5, no. 1, pp. 11–19, 2023, doi: 10.22044/rera.2023.12674.1201.

Bora, D. K., "Green Hydrogen Production with 25 kW Alkaline Electrolyzer Pilot Plant Shows Hydrogen Flow Rate Exponential Behavior with the Stack Current," Preprints, 2025, doi: 10.20944/preprints202507.0445.v1.

de Groot, T. T., "Challenges and Opportunities of Alkaline Water Electrolysis," ECS Meeting Abstracts, MA2023-01, no. 36, pp. 1972–1972, 2023, doi: 10.1149/MA2023-01361972mtgabs.

Dubouis, N., Aymé-Perrot, D., Degoulange, D., Grimaud, A., and Girault, H., "Alkaline electrolyzers: Powering industries and overcoming fundamental challenges," Joule, vol. 8, no. 4, pp. 883–898, 2024, doi: 10.1016/j.joule.2024.02.012.

Esfandiari, N., Aliofkhazraei, M., Colli, A. N., Walsh, F. C., Cherevko, S., Kibler, L. A., Elnagar, M. M., Lund, P. D., Zhang, D., Omanovic, S., and Lee, J., "Metal-based cathodes for hydrogen production by alkaline water electrolysis: Review of materials, degradation mechanism, and durability tests," Progress in Materials Science, vol. 144, 2024, doi: 10.1016/j.pmatsci.2024.101254.

Farmani, A., Fahimi, F., and Nasirpouri, F., "Relationship between degradation mechanism and water electrolysis efficiency of electrodeposited nickel electrodes," npj Materials Degradation, vol. 9, no. 1, pp. 1–16, 2025, doi: 10.1038/s41529-025-00572-z.

Gu, J., Guo, B., Hu, S., Ding, S., Zhang, T., Tian, Z., Yang, F., and Ouyang, M., "Experimental Studies on Dynamic Performance of 250 kW Alkaline Electrolytic System," SSRN Electronic Journal, vol. 17, p. 302, 2023, doi: 10.2139/ssrn.4604062.

Haoran, C., Xia, Y., Wei, W., Yongzhi, Z., Bo, Z., and Leiqi, Z., "Safety and efficiency problems of hydrogen production from alkaline water electrolyzers driven by renewable energy sources," International Journal of Hydrogen Energy, vol. 54, pp. 700–712, 2024, doi: 10.1016/j.ijhydene.2023.08.324.

Hu, S., Guo, B., Ding, S., Yang, F., Dang, J., Liu, B., Gu, J., Ma, J., and Ouyang, M., "A comprehensive review of alkaline water electrolysis mathematical modeling," Applied Energy, vol. 327, p. 120099, 2022, doi: 10.1016/j.apenergy.2022.120099.

Huang, D., Wen, Q., Xiong, B., Lu, A., Ai, X., Zhong, Z., Hu, K., and Fang, J., "Iron Electrodeposition-Induced Degradation on Industrial Alkaline Water Electrolyzer: Multiphysics Model and Economic Analysis," SSRN Electronic Journal, 2024, doi: 10.2139/ssrn.4720710.

Im, S., Kim, W. S., Tamboli, A. M., Sim, J., Jung, Y., Oh, J., and Kim, C.-H., "Preventing Electrode Degradation Against Reverse Current By Interrupting Ion Transfer during Shut-Down in Alkaline Water Electrolysis," ECS Meeting Abstracts, MA2024-02, no. 46, pp. 3228–3228, 2024, doi: 10.1149/ma2024-02463228mtgabs.

Kwon, J., Choi, S., Park, C., Han, H., and Song, T., "Critical challenges and opportunities for the commercialization of alkaline electrolysis: high current density, stability, and safety," Materials Chemistry Frontiers, vol. 8, no. 1, pp. 41–81, 2023, doi: 10.1039/d3qm00730h.

Lindquist, G., "Research and Development Needs to Enable Renewable-Powered Liquid Alkaline Electrolyzers," ECS Meeting Abstracts, MA2024-01, no. 34, pp. 1840–1840, 2024, doi: 10.1149/ma2024-01341840mtgabs.

Maurya, S., Leonard, D. P., and Kang, S. Y., "Investigating Reverse Current Phenomena Induced by Start/Stop Cycling in Lab-Scale Single-Cell Liquid Alkaline Water Electrolyzers," ECS Meeting Abstracts, MA2024-02, no. 45, pp. 3177–3177, 2024, doi: 10.1149/ma2024-02453177mtgabs.

S. AbdelMeguid, H., F. Al-johani, H., F. Saleh, Z., A. Almalki, A., and M. Almalki, A., "Advancing Green Hydrogen Production in Saudi Arabia: Harnessing Solar Energy and Seawater Electrolysis," Clean Energy and Sustainability, vol. 1, no. 1, pp. 1–14, 2023, doi: 10.35534/ces.2023.10006.

Turek, T., Becker, M., Kirstein, F., Gäde, F., Brauns, J., and Lüke, L., "Dynamic Modeling of Liquid Alkaline Water Electrolyzers: From Laboratory Cells to Industrial-Sized Stacks," ECS Meeting Abstracts, MA2024-01, no. 34, pp. 1678–1678, 2024, doi: 10.1149/MA2024-01341678mtgabs.

Tüysüz, H., "Alkaline Water Electrolysis for Green Hydrogen Production," Accounts of Chemical Research, 2023, doi: 10.1021/acs.accounts.3c00709.

Wang, G., Mukundan, R., and Peng, X., "Investigation of Degradation Mechanism of Liquid Alkaline Water Electrolyzer Under Dynamic Operation Condition," ECS Meeting Abstracts, MA2024-02, no. 45, pp. 3178–3178, 2024, doi: 10.1149/ma2024-02453178mtgabs.

Biographies

Hossam AbdelMeguid a professor of thermo-fluid engineering at the Faculty of Engineering, University of Tabuk, Kingdom of Saudi Arabia. He received his Ph.D. in Water Engineering from De Montfort University, UK, in 2011, where his doctoral research focused on Pressure, Leakage, and Energy Management in Water Distribution Systems. He also holds an M.Sc. in Mechanical Engineering from Mansoura University, Egypt, where his award-winning thesis examined Heat Transfer in Microchannels, and a B.Sc. in Mechanical Power Engineering from the same institution.

Dr. AbdelMeguid's research interests span sustainable energy systems, thermal sciences, and water-energy nexus technologies, with particular emphasis on solar-driven desalination, energy storage, and green hydrogen production. He has published and reviewed numerous peer-reviewed papers and has led multidisciplinary projects on solar energy utilization and seawater electrolysis for hydrogen generation in arid regions. At the University of Tabuk, he is actively involved in national and international academic accreditation, curriculum development, and the supervision of undergraduate and postgraduate research projects. His work integrates experimental investigations, techno-economic analysis, and system-level modeling to advance renewable energy applications and to support the Kingdom's vision for a sustainable, low-carbon energy future.

Abdullah Mohammed Al-Mubarak is a Mechanical Engineering student at the University of Tabuk with strong interests in mechanical design, fluid mechanics, and energy systems. Proficient in Autodesk Inventor, he applies 3D modeling, mechanical analysis, and optimization to engineering solutions. His academic background includes thermodynamics, mechanics of materials, and manufacturing processes, providing him with a solid technical foundation. Through academic projects and teamwork, Abdullah has developed practical problem-solving skills and a passion for innovation. Dedicated to advancing sustainable technologies and industrial development, he seeks to apply his expertise to real-world challenges. Motivated by the Kingdom's vision for technological progress, Abdullah aspires to contribute to engineering solutions that promote sustainability and support future national development goals

Omar Bajad Al-Otaibi is a senior undergraduate student in the Department of Mechanical Engineering at the Faculty of Engineering, University of Tabuk, Kingdom of Saudi Arabia. He joined the university in 2021 and has interned at the First Mills Company in Tabuk from 15/06/2025 to 07/08/2025. Engineer Omar Al-Otaibi's interests include design programs such as Inventor and AutoCAD, as well as a keen interest in Arduino. He is also deeply interested in the fields of Material Mechanics, Thermodynamics, and Mechanical Design. Currently, he is involved in a graduation project focusing on green hydrogen production. The project aims to produce hydrogen through solar energy, contributing to the Kingdom of Saudi Arabia's goals for net production.

Abdulrhman Ibrahim Alshaman is a senior Mechanical Engineering student at the University of Tabuk, expected to graduate in 2026. His academic focus is on integrating mechanical systems with renewable energy technologies, particularly green hydrogen production and sustainable design. For his graduation project, he is developing a compact solar-powered electrolyzer with tracking and energy management systems to improve efficiency and cost-effectiveness. His research interests include hydrogen production, sustainable energy systems, aircraft propulsion, solar tracking, and hydraulic and pneumatic systems. During training at First Mills Company – Tabuk Branch, he gained practical experience in mechanical maintenance, industrial operations, and electrical systems. Proficient in MATLAB and Autodesk Inventor, he aims to advance innovative, sustainable technologies supporting the Kingdom's clean energy vision

Husam Alrehaili is the Head of the Department of Mechanical Engineering at the University of Tabuk, Saudi Arabia. He earned his Ph.D. in Mechanical Engineering from Wayne State University (Detroit, USA) in 2024, an M.Sc. in 2018, and a B.Sc. from King Abdulaziz University in 2012. His professional background blends industry and academia: he worked with Saudi Aramco's Berri Gas Plant in mechanical engineering roles and completed training with SABIC (Hadeed) and the Saudi Electricity Company before transitioning to university service. His research interests center on additive manufacturing and alloy development, including laser metal deposition, high-throughput alloy screening, and Ni/Co/Al-based systems; he has developed toolpaths for robotic deposition, designed new alloys, and led experimental campaigns in microstructure–property optimization. In teaching, he has contributed across design and manufacturing—senior capstone, design of machine elements, manufacturing processes, advanced manufacturing, and engineering workshops—while mentoring students in Arduino/controls, CAD/CAM/CAE, and laboratory practice.